DAA/ LANGLEY

SEMIANNUAL STATUS REPORT

MODELING OF TRANSIENT HEAT PIPE OPERATION

By

Gene T. Colwell
James G. Hartley

Prepared for

NATIONAL AERONAUTICS AND SPACE ADMINISTRATION
LANGLEY RESEARCH CENTER
HAMPTON, VIRGINIA 23665

Under

NASA Grant NAG-1-392

June 1986

GEORGIA INSTITUTE OF TECHNOLOGY
A UNIT OF THE UNIVERSITY SYSTEM OF GEORGIA
SCHOOL OF MECHANICAL ENGINEERING
ATLANTA, GEORGIA 30332

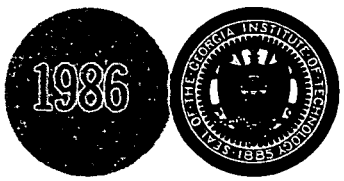

NASA GRANT NAG-1-392

MODELING OF TRANSIENT HEAT PIPE OPERATION

By

Gene T. Colwell and James G. Hartley
School of Mechanical Engineering
Atlanta, Georgia 30332

Submitted to

National Aeronautics and Space Administration
Langley Research Center
Hampton, Virginia 23665

NASA Technical Officer
Charles J. Camarda
Mail Stop 246

Period Covered
August 19, 1985 through February 18, 1986

June 17, 1986

TABLE OF CONTENTS

INTRODUCTION

This report summarizes progress made on NASA Grant NAG-1-392 during the period August 19, 1985 to February 18, 1986. The goal of the project is to develop mathematical models and associated solution procedures which can be used to design heat pipe cooled structures for use on hypersonic vehicles. The models should also have the capibility to predict off-design performance for a variety of operating conditions. It is expected that the resulting models can be used to predict startup behavior of liquid metal heat pipes to be used in reentry vehicles, hypersonic aircraft and space nuclear reactors.

The program work statement includes the following tasks.

I. To investigate the physics of melting and freezing of the working fluid in liquid metal heat pipes, and of other performance limitations which are presently not well understood, and to develop equations, adequate for design, to predict associated performance limits.

II. To evaluate the Langley finite difference heat pipe design computer program and the equations upon which it is based and suggest improvements or additions to upgrade the program.

III. To work with the aerospace contractor who wins the heat pipe study contract to upgrade the contractor's heat pipe analysis capability.

IV. To work with NASA to define the required instrumentation for the heat pipe model which will be built under the heat pipe study contract and to develop a test plan for the heat pipe.

Previous status reports in this series (February 1985 and September 1985) have covered the development of governing differential equations for the startup behavior of initially frozen liquid metal heat pipes. The current

report summarizes work to date related to numerical solutions of governing differential equations for the outer shell and the combination capillary structure and working fluid. The working fluid may be solid (frozen), liquid, or partly liquid and partly solid. Finite element numerical equations using both implicit, explicit and combination methods have been examined. Both enthalpy and specific heat approximations to melting have been examined. The various numerical solutions have been verified using available analytical solutions and experimental data. Work is now in progress aimed at modeling vaporization and condensation processes and behavior of the vapor region during startup. The next status report will cover this work.

GOVERNING DIFFERENTIAL EQUATIONS

The problem under consideration is the initially liquid state at a constant temprature T_o, which is greater than the freezing temperature T_m. For time $t \geq 0$, some surfaces are maintained at a constant temperature T_w that is lower than T_m and the others are insulated. A problem with a phase change of a substance from one state to another is mathematically described as follows

$$C_s \frac{\partial T_s}{\partial t} = \vec{\nabla} \cdot [K_s \vec{\nabla} T_s] \qquad \text{solid region} \qquad (1)$$

$$C_\ell \frac{\partial T_\ell}{\partial t} = \vec{\nabla} \cdot [K_\ell \vec{\nabla} T_\ell] \qquad \text{liquid region} \qquad (2)$$

$$T = T_o \qquad \text{for } t < 0 \qquad (3)$$

$$T = T_w$$

or

$$\frac{\partial T}{\partial n} = 0 \qquad \text{on the boundary surfaces} \tag{4}$$

$$T_s = T_\ell = T_m \tag{5}$$

and

$$K_\ell \frac{\partial T_\ell}{\partial n} - K_s \frac{\partial T_s}{\partial n} = H_{s\ell} \frac{dS}{dt} \qquad \text{on the interface} \tag{6}$$

where subscripts s and ℓ indicate the solid and liquid phases, respectively, and n represents the unit outward normal direction at the interface. Temperatures T_o, T_m, T_w denote respectively the initial, freezing, and boundary tempreaturs. $H_{s\ell}$ is the latent heat of fusion, and S is the interface postion in the X, Y, t domain.

ANALYTICAL SOLUTIONS

The problems of cooling and phase change of semi-infinite body with constant boundary temperature has been solved by several authors. In the present project, these solutions will serve as reference values for numerical calculation.

The Temperature of a Semi-infinite Body

The exact solution to this problem is given by Luikou [1] as

$$\frac{T(x,t) - T_w}{T_o - T_w} = \text{erf}\left(\frac{x}{2(\alpha t)^{1/2}}\right) \tag{7}$$

where

$$\alpha = \frac{K}{\rho C_p}$$

Phase Change of a Semi-infinite Body

The analytical solution of phase change is given by Ozisik [2] as

$$\frac{T_s - T_w}{T_m - T_w} = \frac{\text{erf}[x/2(\alpha_s t)^{1/2}]}{\text{erf}(\lambda)} \qquad \text{for solid region} \qquad (8)$$

$$\frac{T_\ell - T_o}{T_m - T_o} = \frac{\text{erfc}[x/2(\alpha_\ell t)^{1/2}]}{\text{erfc}[\lambda(\alpha_s/\alpha_\ell)^{1/2}]} \qquad \text{for liquid region} \qquad (9)$$

and the location of the interface is

$$\frac{e^{-\lambda^2}}{\text{erf}(\lambda)} + \frac{K_\ell}{K_s}\,\frac{T_m - T_o}{T_m - T_w} \cdot \left(\frac{\alpha_s}{\alpha_\ell}\right)^{1/2} \cdot \frac{e^{-\lambda^2(\alpha_s/\alpha_\ell)}}{\text{erfc}(\lambda(\alpha_s/\alpha_\ell)^{1/2})} = \frac{\lambda H_{s\ell}\sqrt{\pi}}{C_{ps}(T_m - T_w)} \qquad (10)$$

where

$$\lambda = \frac{S(t)}{2(\alpha_s t)^{1/2}}$$

DESCRIPTION OF NUMERICAL METHODS

Finite Element Formulation

The Galerkin weighted residual method is used to derive finite element formulations. Within each element, the unknown function T may be approximated at any time t by the relationship

$$T(x,y,t) = \sum_{i=1}^{n} N_i(x,y) \cdot T_i(t) \qquad (11)$$

where n is the number of nodes assigned to the element, T_i are the descrite nodal values of T, and N_i are the shape functions.

By applying the Galerkin weighted residual method to equations (1) and (2), and sujming the contributions from each element and boundaries, assembly

of the nonlinear transient element equations can be expressed in matrix form as

$$[C]\ \dot{\{T\}} + [K]\ \{T\} = \{F\} \tag{12}$$

where [C] and [K] are, respectively, the capacitance and conductance matrices.

Time-Stepping Techniques

Implicit Method

Let t^n denote a typical time in the response so that $t^{n+1} = t^n + \Delta t$ where Δt is the time increment, and an intermediate time t_m within each time step may be expressed as

$$t_m = t^n + m\Delta t\ ,\quad 0 < m < 1 \tag{13}$$

Then, Equation (12) at t_m is given as

$$[C]\ \dot{\{T\}}_m + [K]\ \{T\}_m = \{F\} \tag{14}$$

By using a Taylor expansion,

$$\{T\}^n = \{T\}_m - \frac{d}{dt}\{T\}_m \cdot (m\Delta t) + \text{High Order Terms} \tag{15}$$

$$\{T\}^{n+1} = \{T\}_m + \frac{d}{dt}\{T\}_m \cdot (m\Delta t) + \text{Higher Order Terms} \tag{16}$$

Subtracting Equation (15) from (16) yields

$$\frac{d}{dt}\{T\}_m = \frac{\{T\}^{n+1} - \{T\}^n}{\Delta t}$$

After the higher order terms of Equation (15) are neglected, substitution of Equation (15) into (17) gives

$$\{T\}_m = (1 - m)\{T\}^n + m\{T\}^{n+1} \tag{18}$$

Substitution of Equation (17) and (18) into the assembly Equation (14) yields

$$\left(\frac{[C]}{\Delta t} + m[K] \right) \{T\}^{n+1} = \left(\frac{[C]}{\Delta t} - (1 - m)[K] \right)\{T\}^n + \{F\} \tag{19}$$

Since the values of [C], [K] and {F} depend on $\{T\}_m$, a choice from among the values m = 0 1/2, 2/3 and 1, respectively, yields explicit Euler forward-difference, Crank-Nicolson center-difference, Galerkin, and fully implicit backward-difference formulations. The fully implicit backward-difference is unconditionally stable and predicts a smooth decay and is therefore chosen with a Newton-Raphson iteration for the implicit method.

Explicit Method

The implicit method is much more stable then the explicit method, but requires an iteration within each time step. To avoid iteration, a three level scheme proposed by Lees [3] was used by Comini et al. [4-8] and Morgan [9]. Oscillations have been observed in certain circumstance, so a slightly modified form was used to improve stability. This method has been used successfully for phase change problems by several investigators.

Another three level scheme is referred to as the DuPont three level schmem. Hogge [10] demonstrated the overall performance of the DuPont method to be superior in accuracy and stability to other time stepping schemes in

solving the one-dimensional homogeneous equation.

Thomas [11] compared several time integration schemes such as the Lees, the DuPont scheme, and Crank-Nicolson method. He concluded that the DuPont three level scheme was clearly superior to that of Lees in both accuracy and stability, and that temperature-dependent terms should be evaluated using $\{T\}^{n+1}$ instead of $\{T\}^{n+3/2}$. By using the DuPont method, Equation (12) can be approximated as

$$\left(\frac{3}{4} [K] + \frac{[C]}{\Delta t} \right) \{T\}^{n+2} = \frac{[C]}{\Delta t} \{T\}^{n+1} + \frac{[K]}{4} \{T\}^{n} + \{F\} \qquad (20)$$

The equations above allow the explicit evaluation of $\{T\}^{n+2}$ without iteration provided that $\{T\}^{n+1}$ and $\{T\}^{n}$ are known. However, this scheme is not self-starting, so $\{T\}^{n+1}$ at the first time step may be calculated by using the implicit method.

Latent Heat Evolution Schemes

The principal difficulties in the analysis of the phase change problem are that the variation of the heat capacity is very rapid at the interface as shown in Figure 1, the position of the moving interface is not known a priori and their shapes may be multi-dimensional. Thus, physically realistic approximation techniques must be used to overcome the difficulties.

It is convient to divide them into two groups, based on the choice of grid used. In the first group, the moving mesh technique continously tracks the location of the interface by deforming the grid system to maintain the finest mesh in the vicinity of the critical phase change region. This technique may be limited to very simple geometries.

In the second group, a fixed grid technique can avoid tracking down the position of the moving interface, but the interface is generally at an unknown

location between nodes. Many different classes of methods are available with the fixed grid sysstem.

The first method uses the enthalpy as a dependent variable along with the temperature, and may be referred to as the enthalpy method. Since two dependent variables are used, the system of algebaric equations are solved by iteration.

The second method treats the latent heat effect accompanying a change of phase in terms of a temperature-dependent specific heat or with the use of an enthalpy function.

These methods avoid the moving interface difficulty so that instead of continously tracking down the position of the moving interface, the same numerical scheme for conduction heat transafer without phase change is equally applicable to the phase change period. Then, the postion of the interface can be easily determined by linear interpolation of nodal temperatures.

Specific Heat Method

This method approximate the rapid variations of heat capacity over the phase change temprature, which is artificially defined, instead of using the Dirac Delta function as shown in Figure 1. Thus, a volumetric heat capacity, which includes the latent heat of phase change, can be expressed as

$$C = \begin{cases} C_s & \text{for } T < T_m - \Delta T \\ C_\ell & \text{for } T > T_m + \Delta T \\ \dfrac{H_{s\ell}}{2\Delta T} + \dfrac{C_s + C_\ell}{2} & \text{for } T_m - \Delta T < T < T_m + \Delta T \end{cases}$$

where ΔT is the phase change temperature interval.

One advantage of the finite element method is the ability to formulate contributions for individual elements before putting them together to

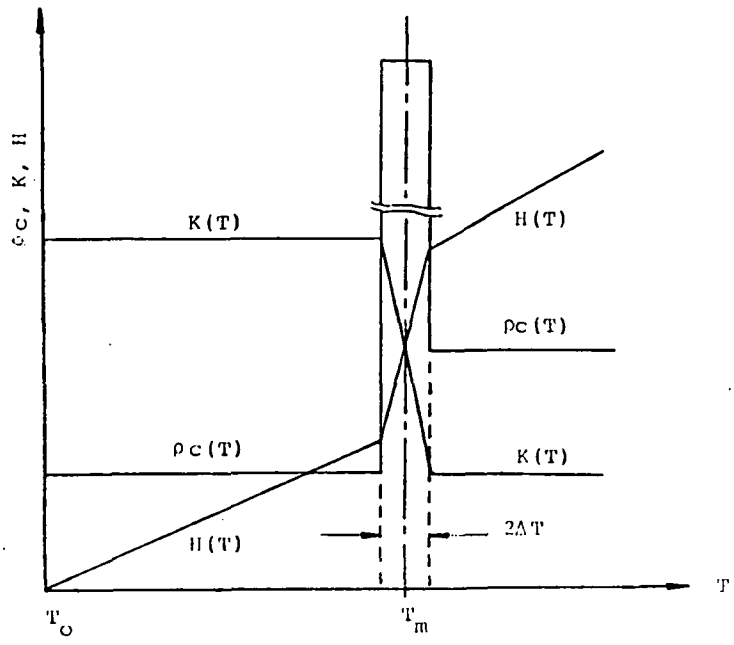

Figure 1. Graphic representation of material of material property variations.

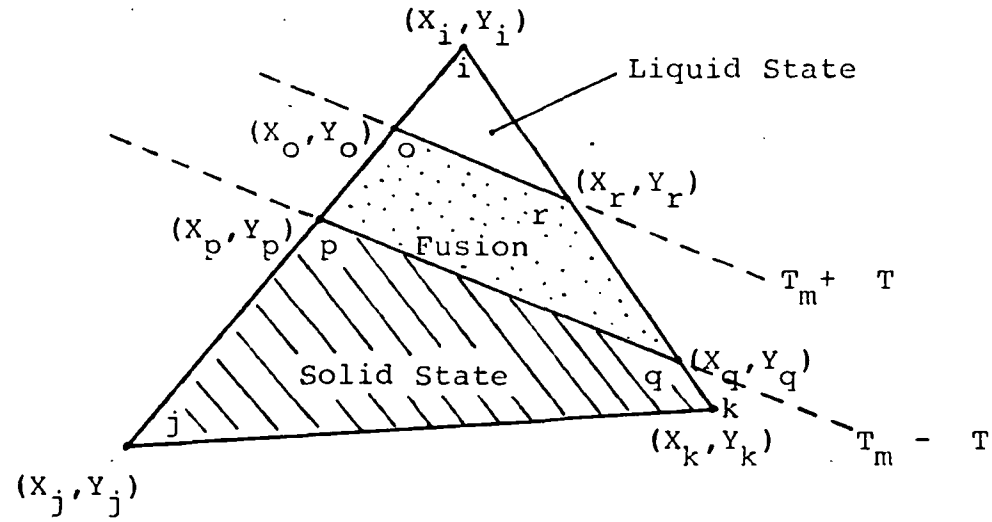

Figure 2. Element Model Showing Solid, Liquid, and Fusion Phase.

represent the entire domain. The individual element characteristics are determined by the shape functions and nodal values. Thus, the heat capacity of the fusion element can be evaluated correctly instead of the direct use of the averaged element temperature.

Consider the phase change element in Figure 2 and assume that the fusion phase is within the element. If the variation of the density of the working substance around the freezing temperature is quite small, the mass fractions can be replaced by area fractions M_ℓ, M_s, M_f for liquid, solid, and fusion phases with unit thickness. Otherwise, mass fractions which are calculated based on the area and density of each phase is employed.

For a linear element, the phases within the element are seperated by the isothermal lines, $T_m + \Delta T$ and $T_m - \Delta T$, passing through the element. The intersecting points of the isothermal lines at the boundaries of the element and nodal points are the vertices of the area occupied by each phase. Since three-node, linear triangular elements are used, at least one of the phases occupies an area having a triangular shape. Then, the area of the traingular is obtained by using the known coordinate values of the vertices of the triangle. For example, the area fracton of the element as shown in Figure 2 are expressed as

$$M_\ell = \pm \frac{1}{2\Delta} \begin{vmatrix} X_i, & Y_i, & 1 \\ X_o, & Y_o, & 1 \\ X_r, & Y_r, & 1 \end{vmatrix}$$

$$M_f = \pm \frac{1}{2\Delta} \begin{vmatrix} X_i, & Y_i, & 1 \\ X_p, & Y_p, & 1 \\ X_q, & Y_q, & 1 \end{vmatrix} - M_\ell$$

$$M_s = 1 - (M_\ell - M_f)$$

where Δ is the total area of the element with the sign chosen so that the area is nonnegative. This new technique, which uses the mass fractions M_ℓ, M_s, M_f for liquid, solid, and fusion phases, is introduced to correct misinterpretation of the specific heat without a vry fine element grid and/or time step.

Enthalpy Function

When temperature approaches the phase change temperature, the heat capacity tends to the Dirac delta function and can not be satisfactorily represented across the peak by any smooth function. In Comini et al [4], a technique based on the integral of heat capacity with respect to temperature is proposed

$$H = \int_{T_\infty}^{T} \rho C \, dT$$

This is a smooth function of temperature in the phase change zone. Therefore, the enthalpy is interpolated rather than the heat capacity in a element as following

$$H = \sum_{i=1}^{n} N_i(X,Y) H_i(t) \qquad (22)$$

where again N_i are the shape functions and H_i are the enthalpy values at nodal points.

From definition, the heat capacity can be expressed as

$$\rho c = dH/dT \qquad (23)$$

Thus, the values of the heat capacity can be approximated by evaluating the gradient of enthalpy with respect to temperature. Defining the direction S to be normal to the interface line, Equation (23) is expressed as

$$\rho c = \left(\frac{\partial H}{\partial S} \Big/ \frac{\partial T}{\partial S} \right)$$

$$= \left(\frac{\partial H}{\partial x} \ell_{sx} + \frac{\partial H}{\partial Y} \ell_{sy} \right) \Big/ \left(\frac{\partial T}{\partial S} \right) \qquad (24)$$

where

$$\ell_{sx} = \frac{\partial T}{\partial x} \Big/ \frac{\partial T}{\partial s} \, , \quad \ell_{sy} = \frac{\partial T}{\partial y} \Big/ \frac{\partial T}{\partial s} \, ,$$

and

$$\frac{\partial T}{\partial s} = \left[\left(\frac{\partial T}{\partial x} \right)^2 + \left(\frac{\partial T}{\partial y} \right)^2 \right]^{1/2}$$

Hence, for the entire element, the final expression of the heat capacity is given as

$$[\rho c] = \left[\frac{\partial H}{\partial x} \cdot \frac{\partial T}{\partial x} + \frac{\partial H}{\partial y} \cdot \frac{\partial T}{\partial y} \right] \Big/ \left[\left(\frac{\partial T}{\partial x} \right)^2 + \left(\frac{\partial T}{\partial y} \right)^2 \right] \qquad (25)$$

where, for linear temperature, tringular element,

$$\frac{\partial H}{\partial x} = \frac{1}{2\Delta} \left(b_1 H_1 + b_2 H_2 + b_3 H_3 \right)$$

$$\frac{\partial H}{\partial Y} = \frac{1}{2\Delta} \left(C_1 H_1 + C_2 H_2 + C_3 H_3 \right)$$

$$\frac{\partial T}{\partial X} = \frac{1}{2\Delta} \left(b_1 T_1 + b_2 T_2 + b_3 T_3 \right)$$

$$\frac{\partial T}{\partial Y} = \frac{1}{2\Delta} \left(C_1 T_1 + C_2 T_2 + C_3 T_3 \right)$$

The appropriate ρc value to be used in the element can be evaluated by Equation (25). This expression is developed by Del-Giudice [12].

Boundary Conditions

Since specified temperature boundary conditions are abruptly imposed on the boundary surface, the temperature gradient at this region is infinite which may cause unstable conditions. This difficulty may be elimilited by introducing a layer of fictitious elements with negligible thermal storage capacity and very high thermal conductivity, such that the temperature gradient at this region artificially becomes of finite value. For this purpose, numerical values of the thermophysical properties of the fictitious layer are chosen as following:

$$\rho c = 1.26 \times 10^4 \text{ J/m}^3 \text{ K}$$

$$k = 4.19 \times 10^3 \text{ W/m K}$$

SOME ILLUSTRATIVE TESTS

Example 1. Temperature of a Semi-Inifinite Body

This example involves pure conduction of heat, without phase change, over a semi-infinite body. It is solved as a two dimensional problem shown in Figure 3. This problem is used to test the general capability of the program written in FORTRAN V.

Adiabatic boundary conditions are assumed throughout but at the face x = 0 the specified boundary temperature (253.0 K) is maintained constant during the entire heat transfer process while the initial solid temperature (283.0 K) is uniform. The conductivity and specific heat are assigned values of aluminum.

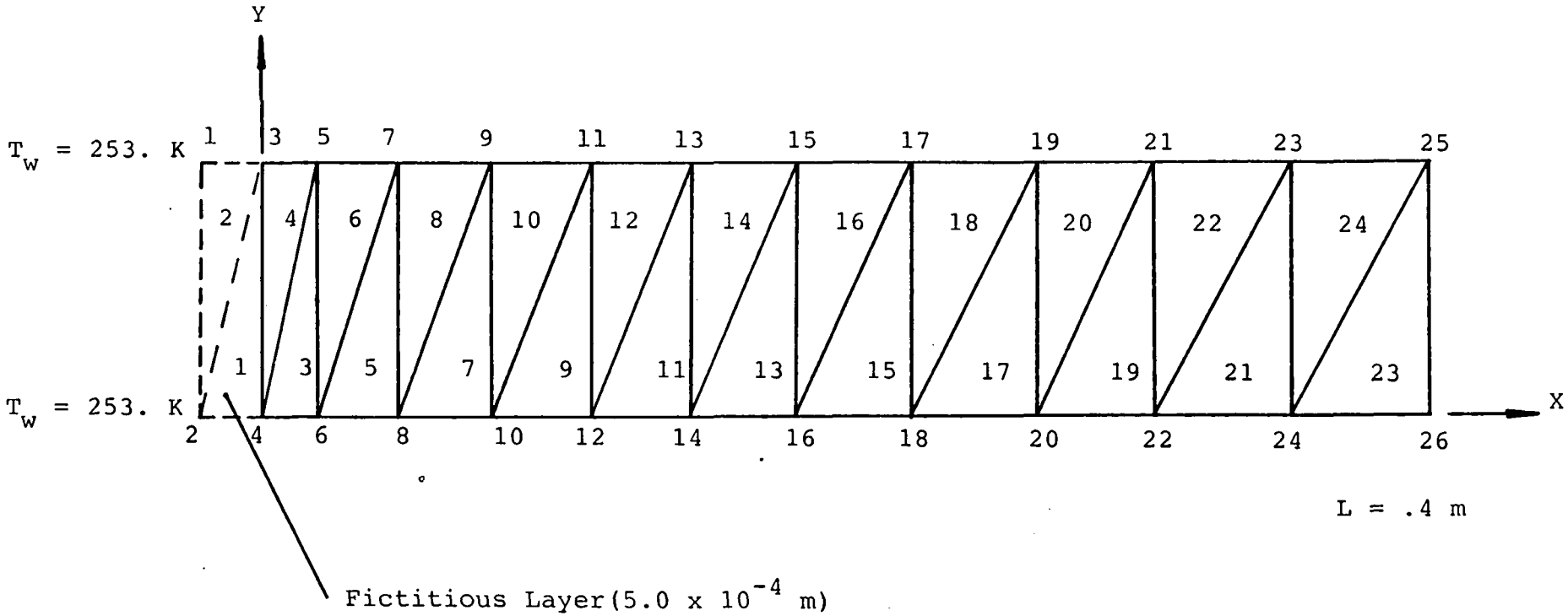

$K_f = 4.19 \times 10^3$ W/m K

K = 93.0 W/m K

$c_f = 1.26 \times 10^4$ J/m^3K

$c = 2.57 \times 10^6$ J/m^3K

$T_{initial}$ = 283 K

Figure 3. Finite-Element mesh for transient conduction heat transfer problem.

Both the fully implicit backward-difference and the explicit time stepping schemes are tested. The explicit scheme causes small oscillations at early time steps. Hence an implicit scheme is employed to eliminate the oscillations in the first five time steps. A time step of 10 seconds is used, and numerical calculations are terminated as asymtotic conditions are approached.

Numerical results are compared in Figure 4 to the well known analytical solution. Both results from the implicit and explicit schemes agree well with the analytical solutions.

Example 2. Solidification of a Semi-Infinite Body in Liquid

This example as represented in Figure 5 tests the ability of the numerical methods to handle the latent heat of phase change which accompanies the discontinuity of the properties at the phase change region.

The same initial temperature and boundary conditions as example 1 are used. The initial temperature is higher than freezing (273.0 K). The properties of water are assigned to the specific heat and conductivities of the solid and the liquid state. The phase change interval, $2\Delta T$ is assumed to be .5 ^{o}K and a time step of 400 seconds is used for Figure 6, 7 and 8.

Numerical results using the specific heat method and the enthalpy function together with a implicit or explicit time stepping scheme are compared with the results from an analytical solution [2] in Figures 6 and 7, respectively. As shown in Figures 6 and 7, the temperature predictions of the solid region by both methods agree well with analytical solutions. In the liquid region, the maximum deviation is about $2^{o}K$.

Numerical results predicted by the explicit method using an implicit scheme for the initial five time steps are closer to the analytical ones than that by the implicit scheme. Also, the explicit method consumes less

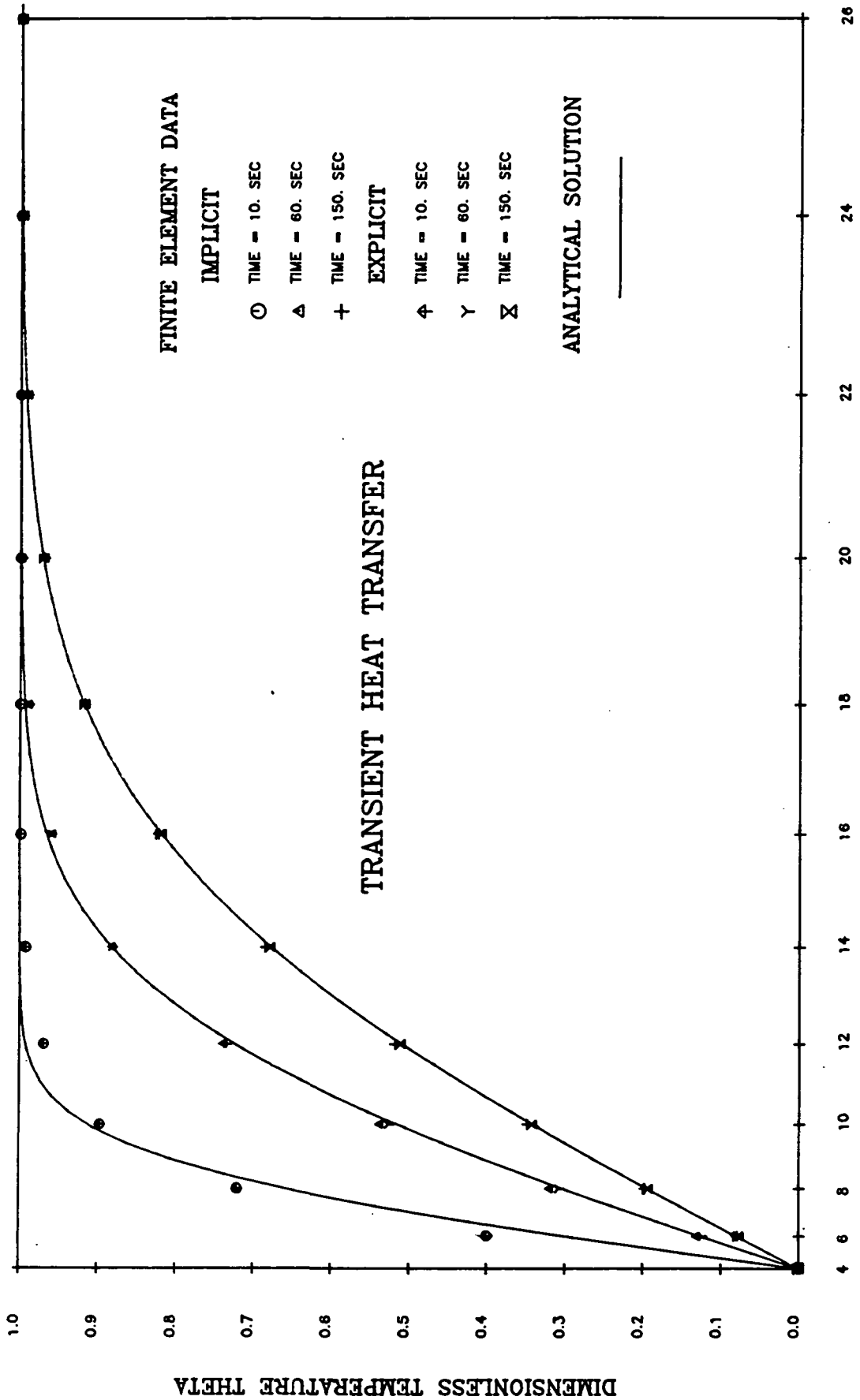

Figure 4. Temperature distribution at different time values; semi-infinite domain. A time step of 10 seconds is used.

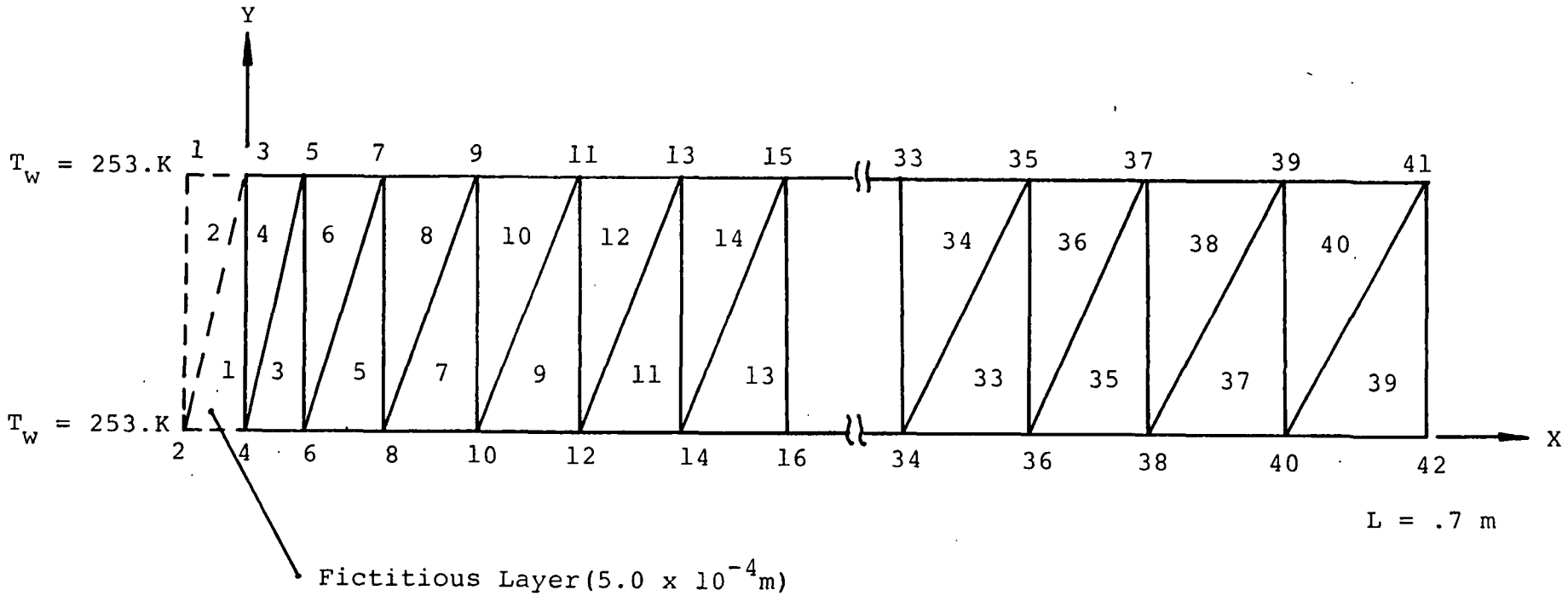

$K_f = 4.19 \times 10^3$ W/m K $\quad K_l = .556$ W/m K $\quad K_s = 2.22$ W/m K

$c_f = 1.26 \times 10^4$ J/m^3K $\quad c_l = 4.226 \times 10^6$ J/m^3K $\quad c_s = 1.762 \times 10^6$ J/m^3K

$T_{initial} = 283$ K

Figure 5. Finite-element mesh for solidification of a slab in liquid.

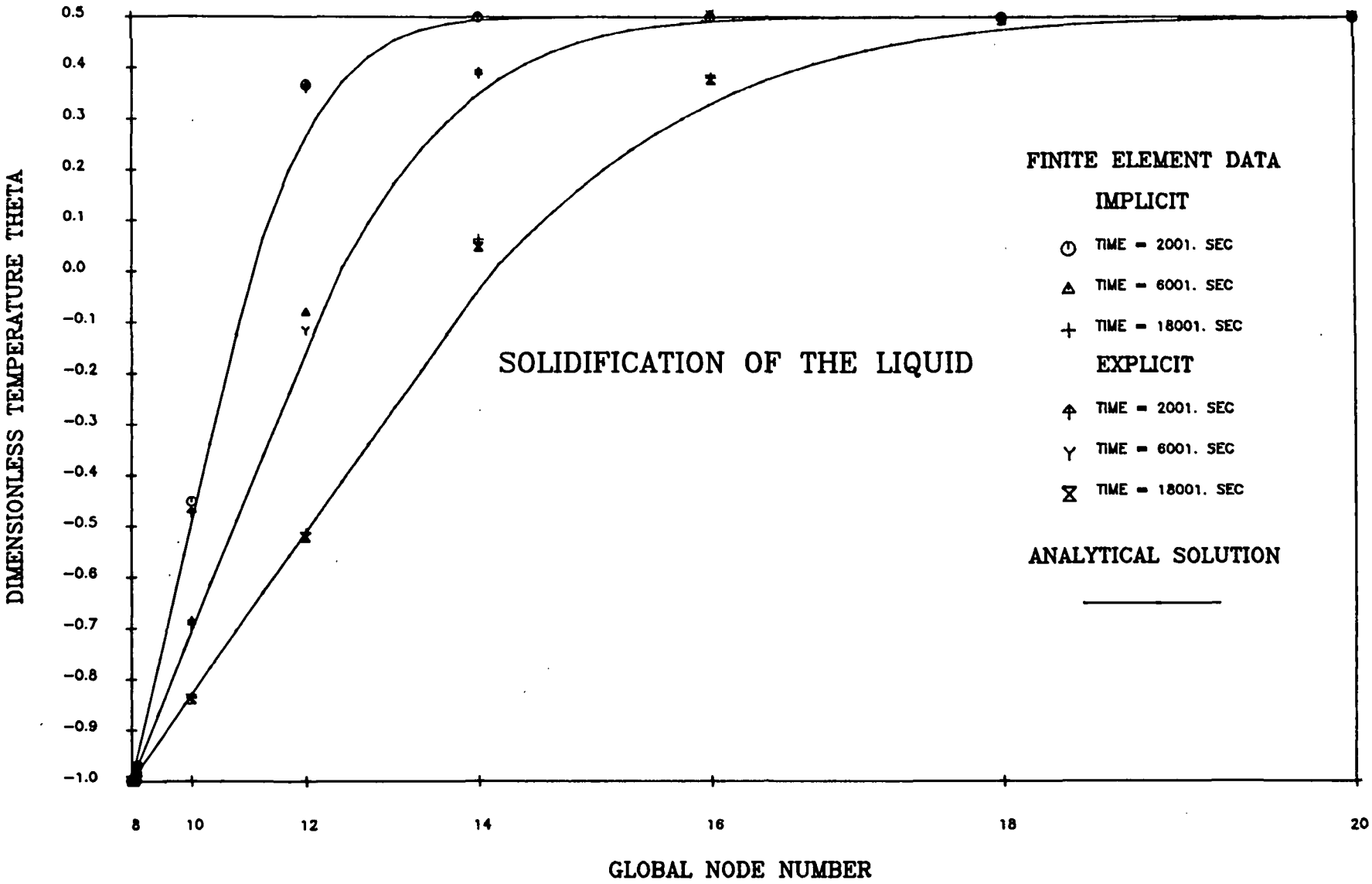

Figure 6. Temperature distributions at different time values during solidification; semi-infinite domain. The latent heat of water is approximated by the specific heat method and a time step of 400 second is used.

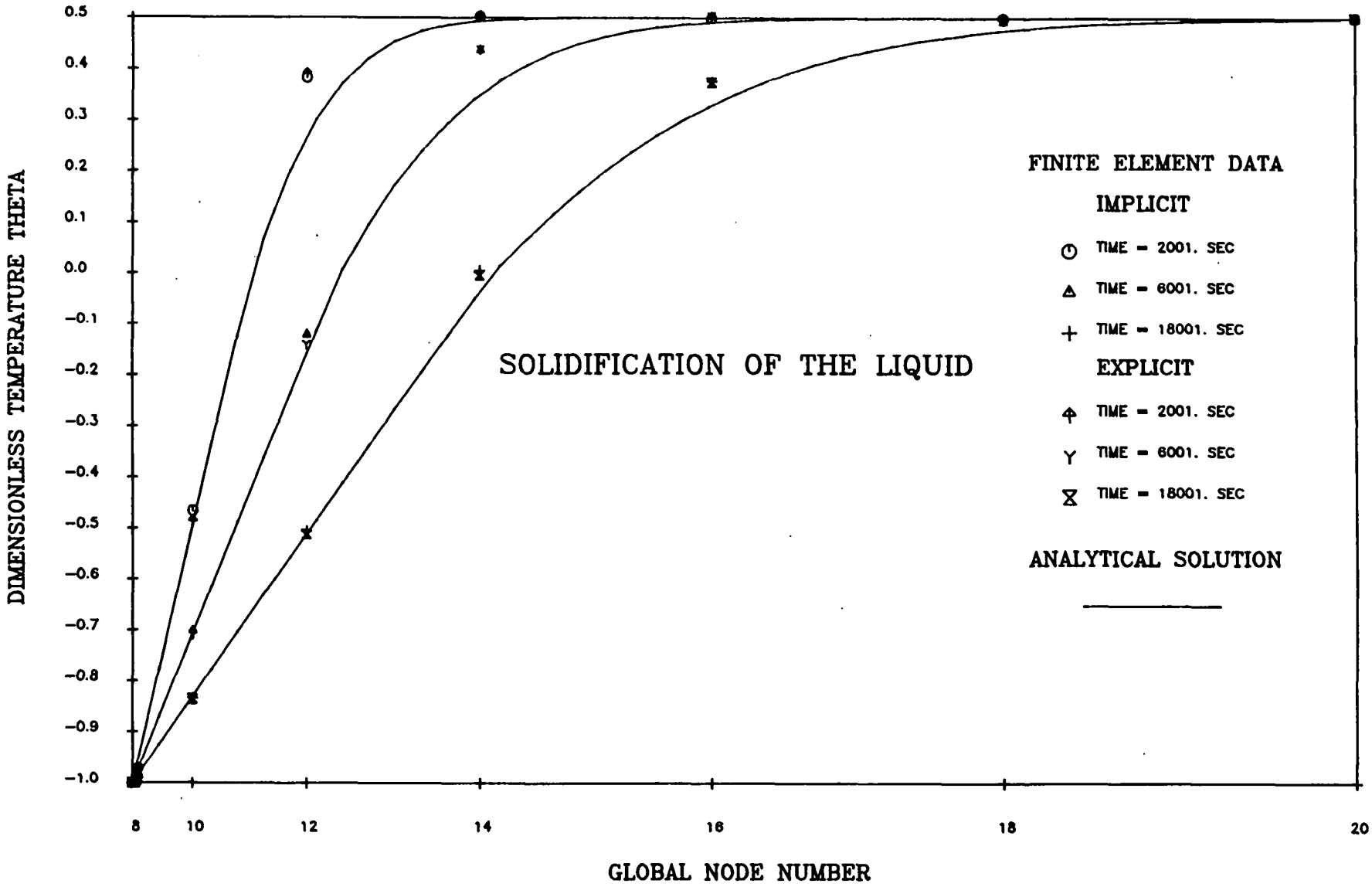

Figure 7. Temperature distributions at different time values during solidification; semi-infinite domain. The latent of water is approximated by the enthalpy function method and a time step of 400 second is used.

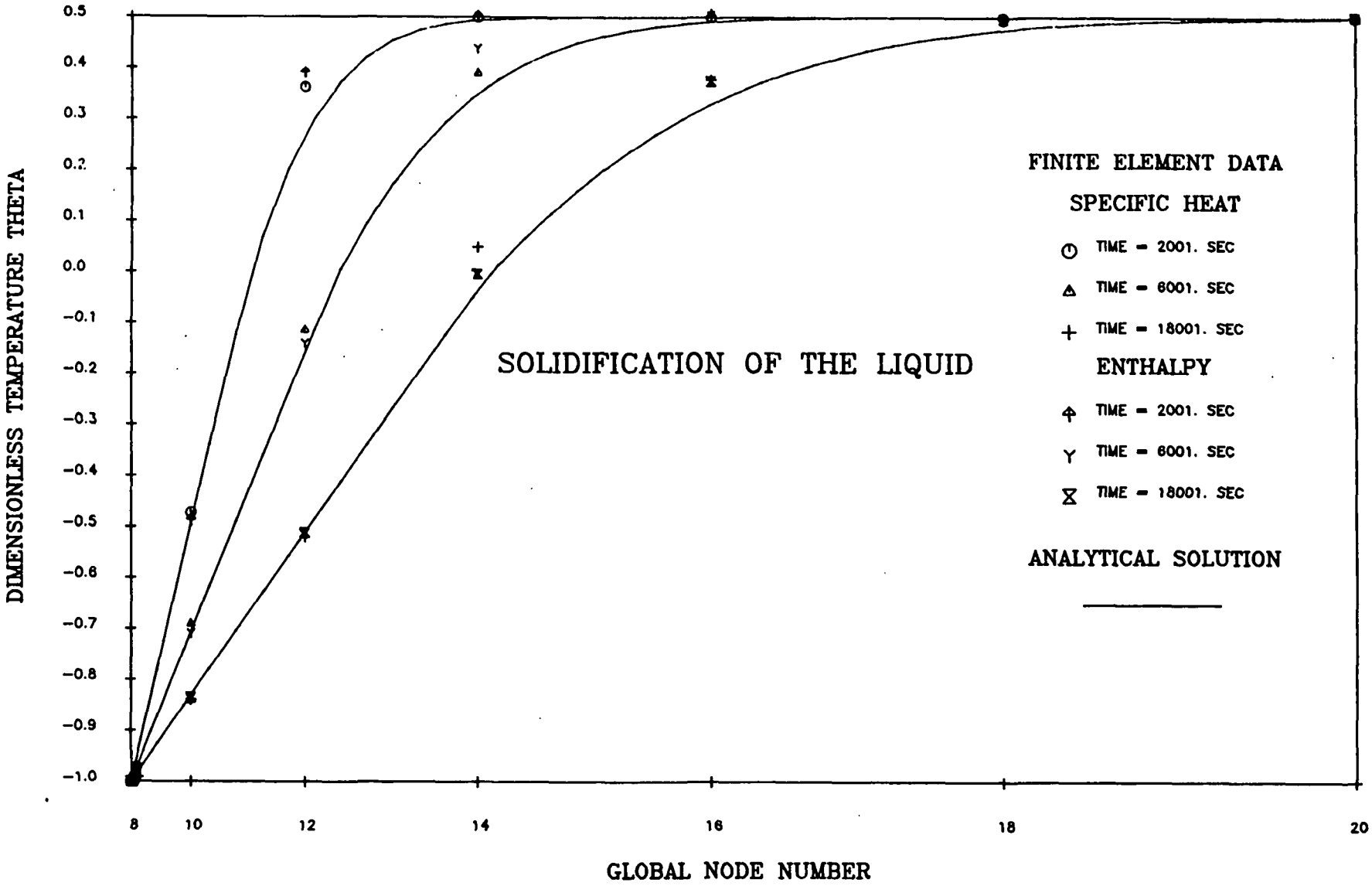

Figure 8. Comparisons of the specific heat and the enthalpy function method with an analytical solution; an explicit time stepping scheme and a time step of 400 seconds are used.

computational time since iteration is not involved.

In Figure 8, numerical results calculated by using specific heat and enthalpy function with an explicit time-stepping scheme are compred with analytical ones. At early time steps, the specific heat method predicts better temprature distributions than that of the enthalpy function but for the later time steps, numerical results predicted by using the enthalpy function gives better agreement to analytical solutions. This method requires much less computational time than the specific heat method. In the solid region, both methods yield quite good results.

To predict temperature distributions for longer time, the enthalpy function with an explicit time scheme are chosen because the results shown in Figures 6, 7 and 8. The same initial and boundary conditions are used, but the domain is extended as shown in Figure 5 and a time step of 500 seconds is used.

The calculated results are compared with analytical solutions in Figure 9. Good prediction is achieved except for the phase change region, but even in this region the maximum deviation is less than 2 K. In Figure 10, the position of interfaces calculated by linear interpolation of adjacent nodal temperatures of the freezing temperature gives good agreement with analytical solutions.

Example 3. Phase Change of Sodium

In this example, sodium is used as the phase change material for one and two-dimensional regions. The initial temperature of the sodium is 393.K which is higher than the freezing temperature (371.K). First kind boundary conditions (293.K) are imposed on boundary surfaces. The phase change interval, $2\Delta T$ is assumed to be 2.K and a time step of 5 seconds is employed. The finite element meshes are shown in Figures 5 and 11.

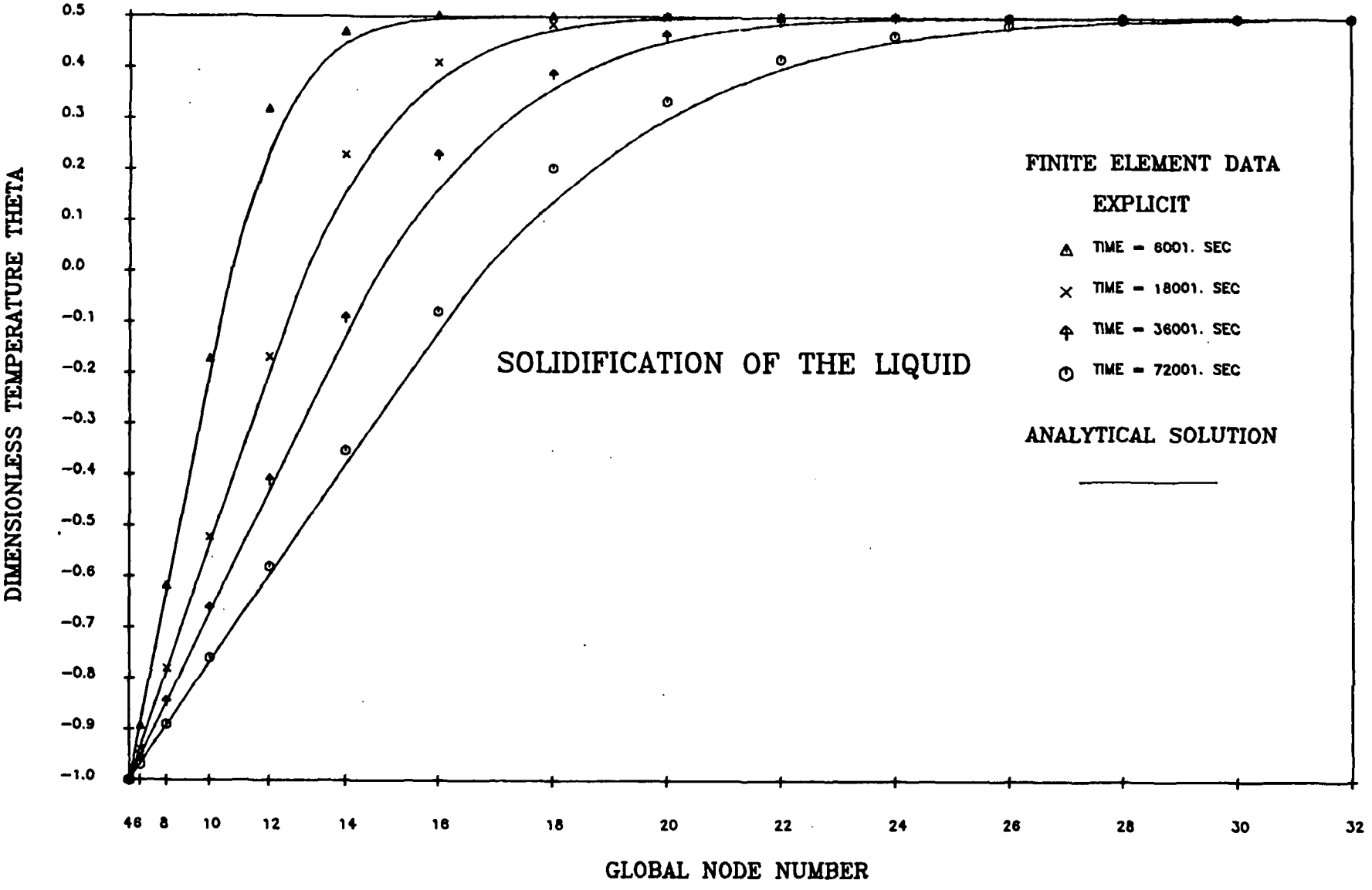

Figure 9. Temperature distributions at different time values during solidification. An enthalpy function and explicit methods with a time step of 500 seconds are used.

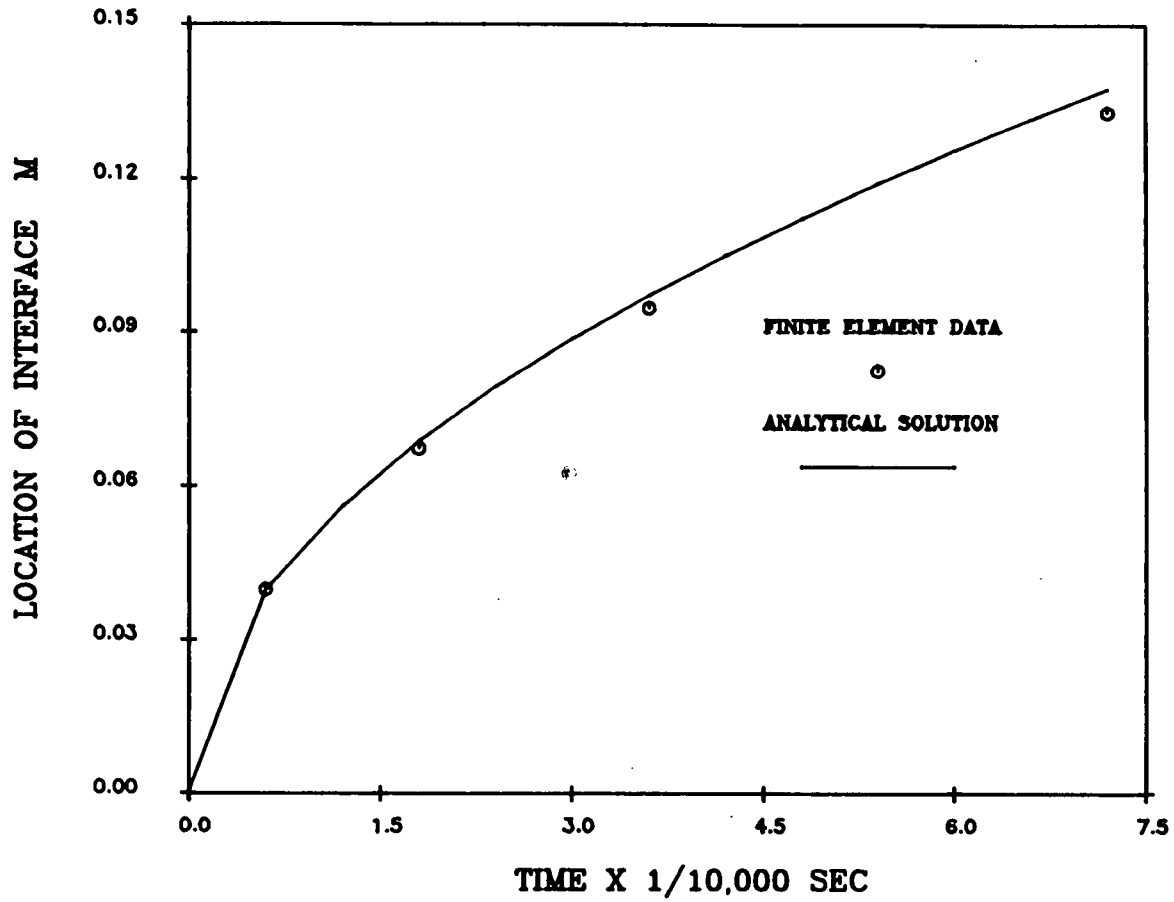

Figure 10. Position of solidification front at different time values referred to in Figure 9.

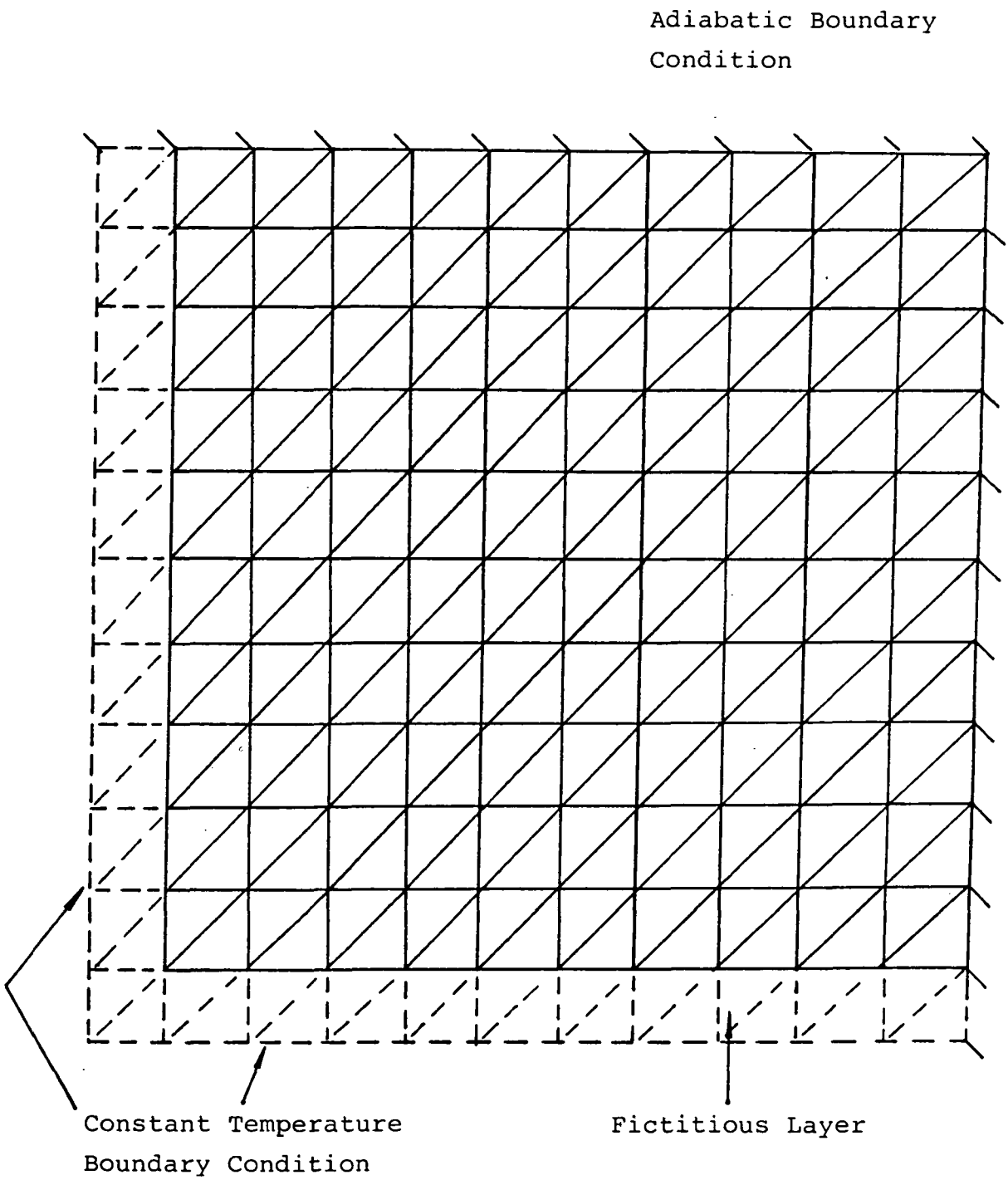

Figure 11. Two-dimensional mesh used to represent a corner region; 242 elements, 144 nodes.

The enthalpy functions with an explicit time stepping scheme is used for the phase change of sodium. In Figures 12 and 13 the temperature distributions for pure conduction and phase change in a one-dimension region show excellent agreement with analytical solutions.

For the two-dimensional case, the position of the interface is compared with an analytical solution given by Jiji [13]. This analytical solution assumes that the ratio of diffusivity for the solid to liquid is unity and that the interface at points beyond three times the one-dimensional stationary interface in x and y directions is the same as the one-dimensional stationary interface position.

Since the ratio of diffusivities is not unity, the numerical solutions can not be directly compared with the analytical solutions. However, as shown in Figure 14, the solutions are close to each other for early time steps because adiabatic boundary conditions at surfaces which do not have first kind boundary conditions are effective for both solutions. The difference of diffusivities relatively small. As time increases the positions of the interface given by numerical calculation advance further than the analytical ones and interface lines obtained from the analytical method are not perpendicular to boundary surfaces. This means that numerical calculations matches adiabatic boundary conditions, but the analytical solution does not. Also, the effect of the difference of diffusivities is not negligible since quite a lot of mass has changed from liquid to solid. Even though numerical solutions do not exactly match analytical solutions because of the different conditions of the problem, general trends of the numerical results are verified.

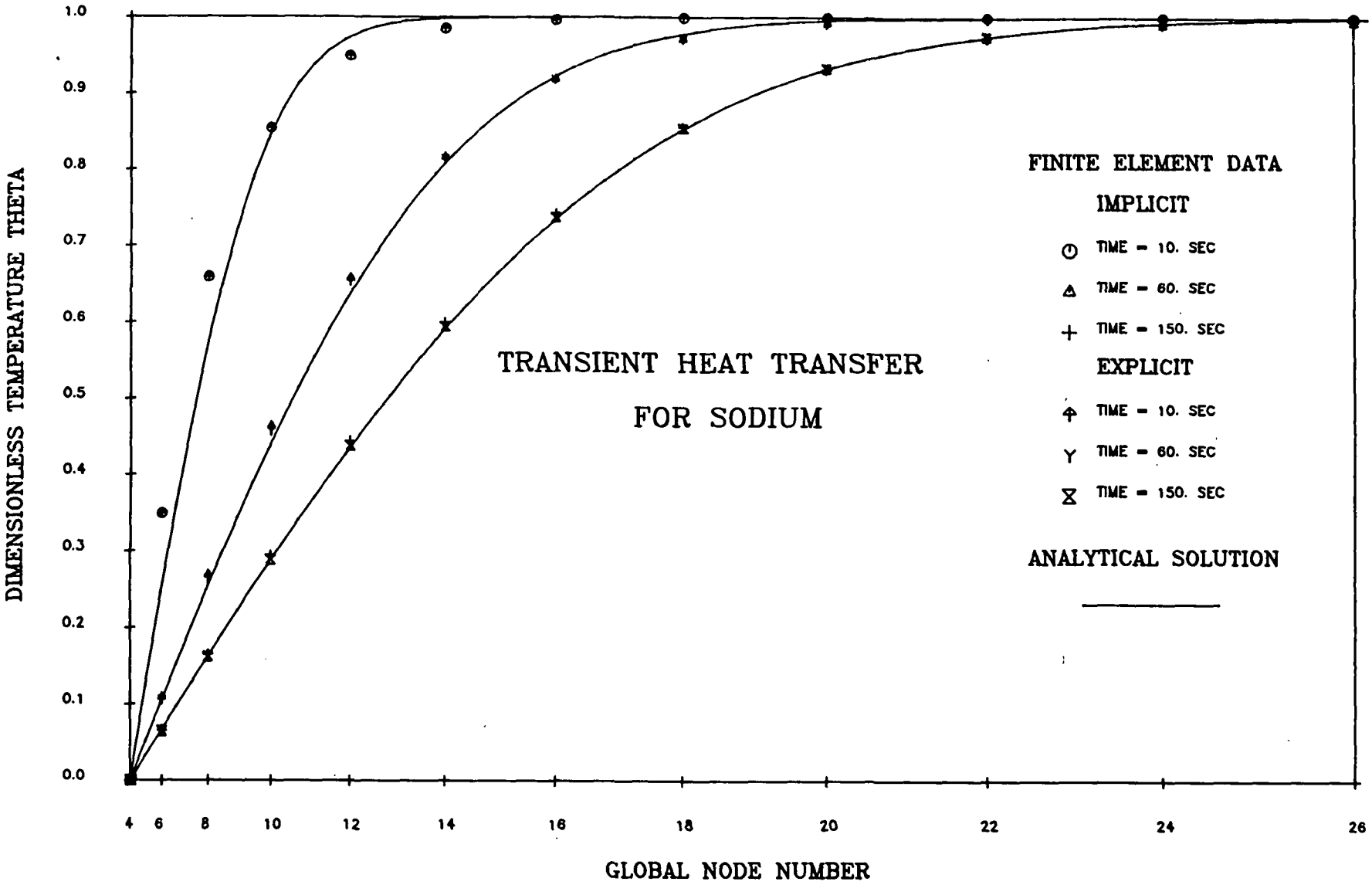

Figure 12. Temperature distribution at different times; semi-inifite domain, time step of 10 seconds is used.

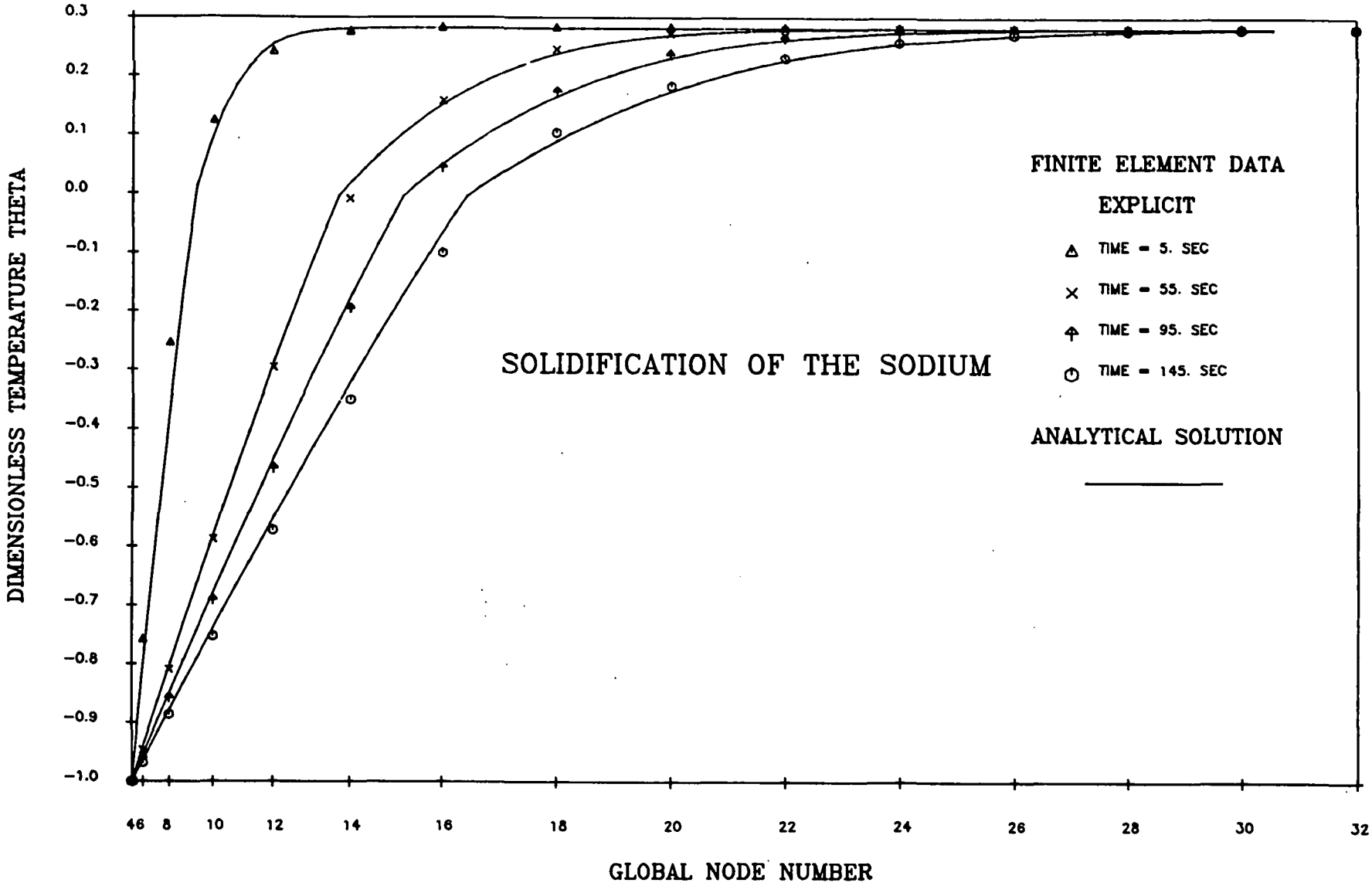

Figure 13. Temperature distribution at different times during the solidification; semi-infinite domain, time step of 5 seconds is used.

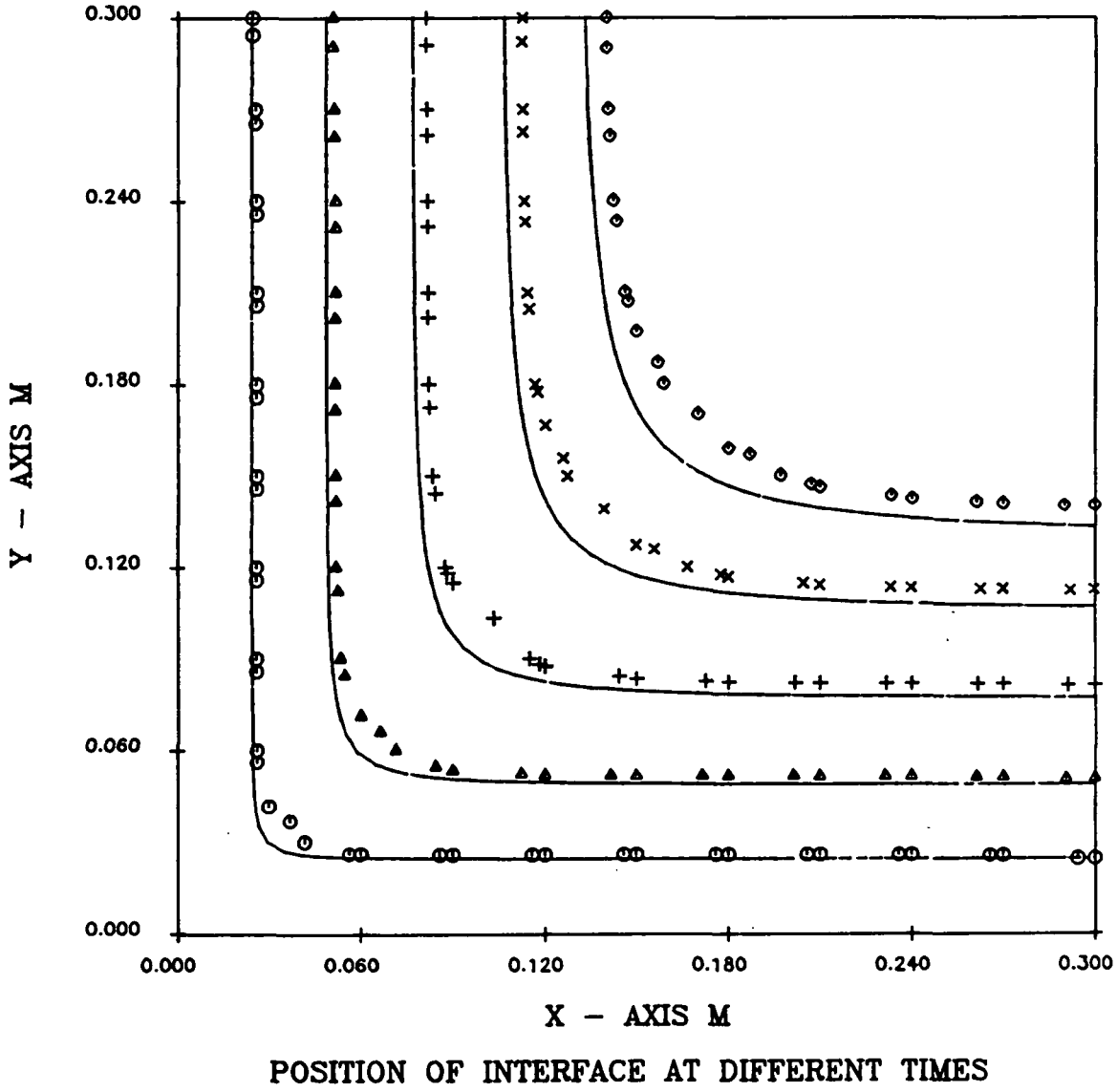

Figure 14. Solidification of sodium in a corner region; position of interface at different times, a time step of 5 seconds is used.

REFERENCES

1. A. V. Luikov, Analytical Heat Diffusion Theory, Academic Press, 1968, pp. 86-89.

2. M. N. Ozisik, Heat Conduction, John Wiley and Son, 1980, pp. 410-415.

3. M. Lees, "A Linear Three-Level Difference Scheme for Quasilinear Parabolic Equations," Maths. Comp. Vol. 20, 1966, pp. 516-522.

4. G. Comini, S. Del Guidice, R. w. Lewis, and O. C. Zienkiewicz, "Finite Element Solution of Non-Linear Heat Conduction Problems with Special Reference to Phase Change," Int. J. Num. Meth. Engng., Vol. 8, 1974, pp. 613-624.

5. G. Comini and R. W. Lewis, "A Numerical Solution of Two-Dimensional Problems Involving Heat and Mass Transfer," Int. J. Heat Mass Trans., Vol. 19, 1976, pp. 1387-1392.

6. G. Comini and S. Del Guidice, "Thermal Aspects of Cryosurgery," J. Heat Trans., Vol. 98, 1976, pp. 543-549.

7. P. E. Frivik, E. Thorbergsen, S. Del Giudice, and G. Comini, "Thermal Design of Pavement Structures in Seasonal Frost Areas," J. Heat Trans., Vol. 99, 1977, pp. 533-540.

8. P. E. Frivik, G. Comini, "Seepage and Heat Flow in Soil Freezing," J. Heat Trans., Vol. 104, 1982, pp. 323-328.

9. K. Morgan, R. W. Lewis, and O. C. Zienkiewicz, "An Improved Algorithm for Heat Conduction Problems with Phase Change," Int. J. Num. Meth. Engng., Vol. 12, 1978, pp. 1191-1195.

10. M. A. Hogge, "A Comparison of Two- and Three-Level Integration Schemes for Non-Linear Heat Conduction," Num. Meth. Heat Trans., R. W. Lewis et al. eds., John Wiley and Son Ltd., 1981, pp. 75-90.

11. B. G. Thomas, I. V. Samarasekera, and J. K. Brimacombe, "Comparison of Numerical Modeling Techniques for Complex, Two-Dimensional, Transient Heat Conduction Problems," Metallurgical Transactions B, Vol. 15B, No. 2, 1984, pp. 307-318.

12. S. Del Giudice, G. Comini, and R. Lewis, "Finite Element Simulation of Freezing Processes in Solid," Int. J. Numerical and Analytical Methods Geomechanics, 1978, Vol. 2, pp. 223-235.

13. K. A. Rathjen and L. M. Jiji, "Heat Conduction with Melting or Freezing in a Corner", J. of Heat Transfer, Feb. 1971, pp. 101-109.